



Schematic of mean thickness distribution on the lateral aspect of the canine frontal sinus as an experimental model of sinus surgery

Jung-Hee Bae^{1,*}, Han-Seok Kim^{2,*}, Sung-Yoon Won³, Da-Hye Kim¹, Ui-Won Jung⁴, Hee-Jin Kim², Kyung-Seok Hu²

¹Department of Dental Hygiene, Division of Health Science, Dongseo University, Busan, ²Division in Anatomy and Developmental Biology, Department of Oral Biology, Yonsei University College of Dentistry, Seoul, ³Department of Occupational Therapy, College of Health and Welfare, Semyung University, Jecheon, ⁴Department of Periodontology, Research Institute for Periodontal Regeneration, Yonsei University College of Dentistry, Seoul, Korea

Abstract: The dog frontal sinus may represent an alternative model dental implant research; its topographical resemblance to the maxillary sinus renders it a potentially favorable experimental environment. The aim of this study was thus to elucidate the anatomical configuration of the canine frontal sinus and histological characteristics, and to determine whether it could be a new canine experimental model for dental implant research. Twenty-four sides of canine frontal bones were harvested. The distance from the nasion to the emerging point of the lateral aspect of the canine frontal sinus was measured with the aid of Lucion software. The thicknesses of the canine frontal sinus wall were measured, and the two specimens stained with hematoxylin and eosin. The mean distance from the nasion to the emerging point of the lateral aspect of the canine frontal sinus was 16.0 mm. The mean thicknesses of the canine frontal bone at 3, 6, 9, 12, and 15 mm lateral to the midsagittal plane were 2.3, 2.7, 3.2, 3.8, and 3.7 mm, respectively. The canine frontal sinus was lined with pseudostratified ciliated columnar epithelium. These data suggest that the canine frontal sinus is a suitable alternative to the canine maxillary sinus as a model for studying various sinus augmentation protocols.

Key words: Sinus augmentation, Frontal sinus, Dog, Experimental study, Implantation

Received May 12, 2018; Revised August 8, 2018; Accepted August 8, 2018

Introduction

Dental implant placement has been established as one of the most favorable treatment options for edentulous area. In the early researches about dental implant, the material

properties, mechanical features and surface modification of titanium fixtures were investigated [1, 2]. Validity of various restorative modalities using dental implants was also studied [3, 4]. In the posterior maxilla, sinus floor elevation is implemented widely to overcome unfavorable anatomical conditions on which standard length implants could not be placed [5-7].

To overcome unfavorable anatomic conditions such as pneumatization of maxillary sinus, alveolar ridge or bony defect around implant, various animal models have been experimented [8-13]. The most explicit and definite findings can be only obtained by histological evaluation of tissues around dental implant. Harvesting human specimens around dental implant is usually not possible due to ethical issue. Thus,

Corresponding author:

Kyung-Seok Hu
Division in Anatomy and Developmental Biology, Department of Oral Biology, Yonsei University College of Dentistry, 50-1 Yonsei-ro, Seodaemun-gu, Seoul 03722, Korea
Tel: +82-2-2228-3047, Fax: +82-2-393-8076, E-mail: hks318@yuhs.ac

*Jung-Hee Bae and Han-Seok Kim contributed equally to this work.

Copyright © 2018. Anatomy & Cell Biology

This is an Open Access article distributed under the terms of the Creative Commons Attribution Non-Commercial License (<http://creativecommons.org/licenses/by-nc/4.0/>) which permits unrestricted non-commercial use, distribution, and reproduction in any medium, provided the original work is properly cited.

experiments and observations using animals are needed to provide valuable histological data regarding cellular responses to dental fixtures.

Many studies about maxillary sinus for dental implant placement were performed in animals; dog, sheep, rabbit, goat, and monkey [8-12]. Sheep, goats, and monkeys are expensive and difficult to be managed for research, whereas animal such as rabbit and dog is relatively inexpensive [14]. In particular, dogs are widely used as experimental subjects in maxillofacial surgery and orthopedic surgery research [15]. The similarity of the respiratory epithelia and maxillary sinus membrane between humans and dogs renders the latter as potentially suitable subjects for sinus research [16]. In addition, the canine model is easy to maintain, durable, relatively resistant to infection, and of an appropriate size for dental implant experiments [8]. However, the canine maxillary sinus is difficult to be approached and too small to be manipulated for dental implant placement.

A possible alternative to the maxillary sinus for research can be the frontal sinus in dogs, since its topographical resemblance to the maxillary sinus would serve as a favorable experimental environment. Few dental implant studies have been performed on the canine frontal sinus because the anatomical structure of the canine frontal sinus is not well known [17]. The frontal sinus can be used effectively for dental implant research if detailed anatomical information is available regarding the positional variations in its thickness.

Therefore, the aim of this study was thus to elucidate the anatomical configuration of the canine frontal sinus, and in particular its thickness at various locations and histological characteristics, with a view to establishing its usefulness as a canine experimental model for dental implant research.

Materials and Methods

Materials

Twenty-four sides of canine frontal bones were harvested from the carcass of mongrel dogs (20–25 kg body weight) for use in the present study. The soft tissues overlying the frontal bone surface were eliminated, and only undamaged specimens were included in the study. One side of the canine frontal sinus was regarded as a specimen, and no distinction was made between right and left specimens.

Methods

Morphology of the frontal sinus using micro-CT

The specimens were scanned with a micro-CT system (Skyscan 1076, Skyscan, Antwerp, Belgium). A specimen was placed on the holder between the X-ray source and the CCD camera and kept in the field of view; it was then rotated around the vertical axis at intervals of 0.9° for 180° , producing 200 projections. The X-ray beam was projected onto a phosphorus screen, which converted the X-rays into visible light that could be detected by the CCD camera. The collected data were then digitized by a frame grabber and transmitted to a computer running topographic reconstruction software. Serial two dimensional images obtained by micro-CT were cross-sectional $1,968 \times 1,968$ pixel images. A three dimensional structural image with voxels of size $35 \mu\text{m} \times 35 \mu\text{m} \times 35 \mu\text{m}$ was reconstructed from the two dimensional images (with pixels of $35 \text{mm} \times 35 \text{mm}$).

The lateral aspect of the canine frontal sinus was used for observation in this study, because the rostral and medial frontal sinuses are too narrow to be used for implant placement. After the reconstruction procedure, the distance from the nasion to the emerging point of the lateral aspect of the canine frontal sinus was measured with the aid of Lucion software (version 1.2, CyberMed, Seoul, Korea) (Fig. 1).

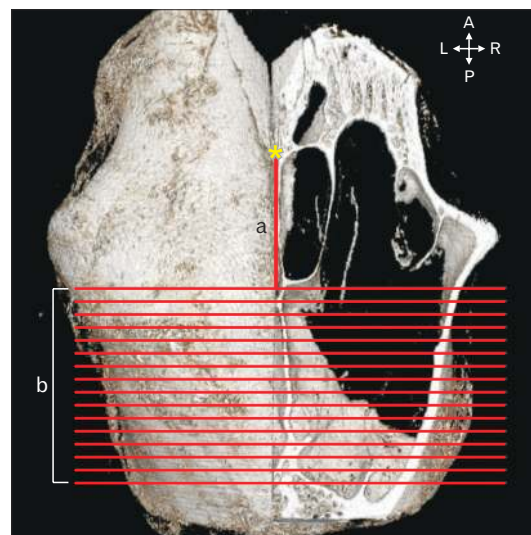


Fig. 1. Parameters measured in the canine frontal bone and sinus with the aid of Lucion software. a, the distance from nasion (yellow asterisk) to the emerging point of the lateral aspect of the canine frontal sinus; b, the 16 coronal sections imaged from the emerging point of the lateral aspect of the canine frontal sinus in the posterior direction at 1-mm intervals. A, anterior; P, posterior; L, left; R, right.

The specimens were sectioned in the coronal plane from the emerging point of the lateral aspect of the canine frontal sinus, posteriorly at 1-mm intervals, and named coronal sectioned image CS1 (the emerging point of the lateral aspect of the canine frontal sinus) to CS16 (the 16th coronal section that was 16 mm posterior to CS1) (b in Fig. 1). The thickness of the canine frontal sinus wall was measured at distances of 3, 6, 9, 12, and 15 mm from the midsagittal plane in images CS1–CS16 using the Lucion software (Fig. 2). The mean and standard deviation values were calculated for each point for all specimens (n=24) using Microsoft Office Excel (Microsoft, Redmond, WA, USA). The values were compared according to their lateral and posterior locations.

Histologic findings

The lateral aspect of the canine frontal sinus was decalcified in 10% nitric acid (B96771, Duksan Pure Chemicals, Ansan, Korea) over a period of about 2 weeks. The samples were fixed for 72 hours with 4% paraformaldehyde, embedded in paraffin wax, sectioned at a thickness of 7 μ m, and then stained with hematoxylin and eosin. Histological observations were performed with the aid of a light microscope, and photographs were taken using the Leica Microsystem CTR 6000 device (Leica, Wetzlar, Germany).

Results

The distance from the nasion to the emerging point of the lateral aspect of the canine frontal sinus

There were septa within the frontal sinus between the nasion and the emerging point of the lateral aspect of the

canine frontal sinus. The mean distance from the nasion to the emerging point of the lateral aspect of the canine frontal sinus was 16.0 mm (range, 10.2–23.0 mm). The emerging point of the lateral aspect of the canine frontal sinus differed significantly depending on the location of the septa within the frontal sinus.

The thickness of the outer table of the frontal bone

The mean thicknesses of the outer table of the canine frontal bone (Table 1) at 3, 6, 9, 12, and 15 mm lateral to the midsagittal plane were 2.3 mm (range, 2.0–2.7 mm), 2.7 mm (range, 2.5–3.4 mm), 3.2 mm (range, 2.9–3.9 mm), 3.8 mm (range, 3.1–4.2 mm), and 3.7 mm (range, 3.2–4.0 mm), respectively. The mean thickness at 15 mm was 1.6 times greater than that at 3 mm (Fig. 3).

At 3, 6, and 9 mm lateral to the midsagittal plane, the thickness tended to increase slightly from CS1 to CS16. At 12 and 15 mm lateral to the midsagittal plane, some differences in thickness were observed from CS1 to CS16. At 12 mm, the thickness tended to increase from CS1 to CS8 and from CS11 to CS16, and to decrease from CS8 to CS11. At 15mm, the thickness tended to increase from CS1 to CS8, and to be constant from CS8 to CS16.

The thickest region was from the nasion 7–8 and 14–16 mm posteriorly and from the midsagittal plane 12 mm later-

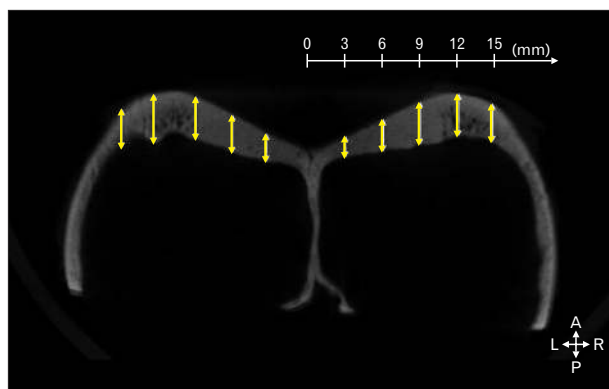


Fig. 2. The thickness of the canine frontal bone was measured at 3, 6, 9, 12, and 15 mm lateral to the midsagittal plane (double-headed arrows) at 3-mm intervals on each coronally sectioned image (CS1–CS16). A, anterior; P, posterior; L, left; R, right.

Table 1. Mean thickness of the outer table of the canine frontal bone from nasion to the emerging point of the lateral aspect of the canine frontal sinus

| | Thickness (mm) | | | | |
|-------|----------------|---------|---------|---------|---------|
| | 3 | 6 | 9 | 12 | 15 |
| CS 1 | 2.1±0.4 | 2.6±0.7 | 3.0±1.0 | 3.1±1.0 | 3.2±0.9 |
| CS 2 | 2.1±0.5 | 2.5±0.8 | 2.9±1.1 | 3.3±1.1 | 3.3±1.1 |
| CS 3 | 2.0±0.4 | 2.6±0.8 | 3.0±1.0 | 3.6±1.3 | 3.5±1.0 |
| CS 4 | 2.0±0.5 | 2.7±0.7 | 3.1±1.1 | 3.7±1.3 | 3.8±1.2 |
| CS 5 | 2.1±0.6 | 2.7±0.8 | 3.1±1.0 | 3.8±1.3 | 3.9±1.2 |
| CS 6 | 2.2±0.6 | 2.7±0.7 | 3.3±1.1 | 3.9±1.3 | 4.0±1.3 |
| CS 7 | 2.2±0.6 | 2.7±0.8 | 3.3±1.2 | 4.1±1.3 | 4.0±1.2 |
| CS 8 | 2.2±0.6 | 2.8±0.9 | 3.5±1.0 | 4.2±1.3 | 4.0±1.3 |
| CS 9 | 2.2±0.8 | 2.8±0.9 | 3.4±1.2 | 3.8±1.1 | 3.8±1.4 |
| CS 10 | 2.3±0.8 | 2.8±1.0 | 3.6±1.1 | 3.8±1.2 | 3.8±1.3 |
| CS 11 | 2.4±0.9 | 3.1±0.9 | 3.6±1.3 | 3.7±1.2 | 3.7±1.3 |
| CS 12 | 2.5±1.0 | 3.1±1.1 | 3.7±1.2 | 3.8±1.3 | 3.8±1.3 |
| CS 13 | 2.6±1.0 | 3.3±1.1 | 3.7±1.2 | 3.8±1.3 | 3.7±1.5 |
| CS 14 | 2.6±1.1 | 3.3±1.2 | 3.8±1.2 | 4.0±1.4 | 3.7±1.7 |
| CS 15 | 2.7±1.0 | 3.5±1.2 | 3.9±1.2 | 4.0±1.5 | 3.8±1.8 |
| CS 16 | 2.7±1.0 | 3.4±1.2 | 3.9±1.3 | 4.0±1.6 | 3.6±1.6 |

Values are presented as mean±standard deviation. CS1–CS16, the coronal section images from the emerging point of the lateral aspect of the canine frontal sinus to the posterior direction at intervals of 1 mm; 3, 6, 9, 12, and 15 mm, from the midsagittal plane to lateral direction at intervals of 3 mm in each coronal sectioned image.

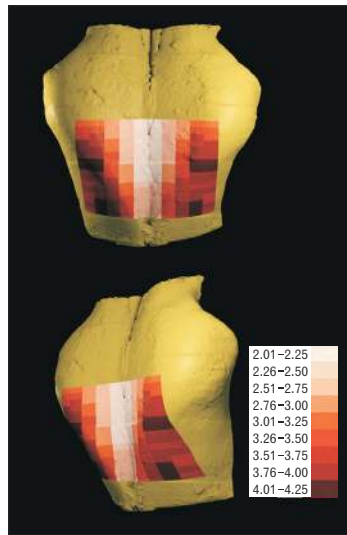


Fig. 3. The thickness of the canine frontal sinus wall (mm).

ally (range, 4.0–4.2 mm), and from the nasion 6–8 mm posteriorly and from the midsagittal plane 15 mm laterally (4.0 mm). The thinnest region was from the midsagittal plane 3 mm laterally (range, 2.1–2.7 mm). In general, there was a tendency toward a greater thickness on proceeding laterally from the midsagittal plane and on proceeding posteriorly from the nasion.

Histological findings

The microscopic examination of the internal side of the canine sinus demonstrated that the lining epithelium comprised layers of nonkeratinized epithelium, basement membrane, and lamina propria. Ciliated epithelium was observed lining the internal surface of the sinus (Fig. 4A). There was a distinctly stained line of tight junctions, and the cilia of the outer epithelium were observed on the outside of that line. The eosinophilic cytoplasmic area was located below the tight-junction line. A nuclear column typically comprising 5–10 cells was found between the tight-junction line and the basement membrane, arranged vertically. Since the nucleus of the outmost cell was squashed horizontally in the stratified epithelium, the nuclear column of the canine sinus lining epithelium was considered as pseudostratified rather than stratified. The epithelial cells overlapped, and the nucleus was superimposed in the image, revealing a vertically stratified arrangement. The lamina propria was observed below the basement membrane, and the vasculature was found among the cells of the lamina propria. Goblet cells were observed among the epithelial cells in higher magnification images (Fig.

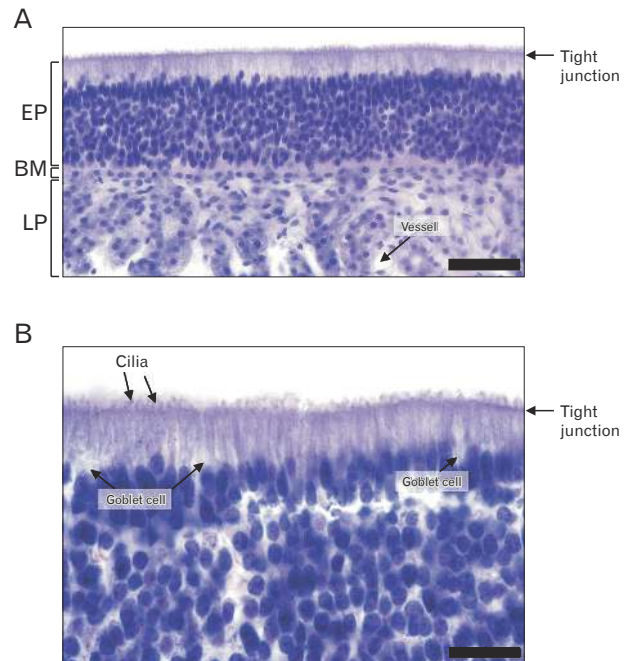


Fig. 4. Histological examination of the canine frontal sinus mucosa (A, $\times 400$; B, $\times 1,000$). Scale bars=50 μm (A), 200 μm (B). EP, epithelium; BM, basement membrane; LP, lamina propria.

4B). Notably, the cilia of the epithelial cells were outside the tight junction line. Microscope images showed that the canine frontal sinus was lined by a pseudostratified ciliated columnar epithelium, comprising cilia and abundant single layered cells in a manner suggestive of multiple cell layers comprising goblet cells.

Discussion

The canine frontal sinus comprises the inner and outer tables of the anterior end of the frontal bone and three compartments of air cavities located within these bony tables: the rostral, medial, and lateral frontal sinuses. The lateral aspect of the canine frontal sinus, which is the largest of the frontal sinuses, extends into the zygomatic process of the frontal bone [18]. In general, animal model should have a proper cortical thickness in the lateral wall, a similar morphology and resistance of the sinus membrane in humans, and an oral approach [19]. At based our results, the canine frontal sinus offers several advantages as a model for studying sinus augmentation and its related interventions.

The main advantage of the canine frontal sinus is the extraoral approach which is no necessity for tooth extraction before implantation. Usually, when animal experiment was

performed for implantation, the teeth were extracted. After extraction, the healing period was needed for 3–6 months [16]. Bretan et al. [20] described the method to approach the canine frontal sinus. First, two straight lines were drawn: one along the medial line of the frontal region; and the other at 45° from the pupil. At the intersection point, 1–1.5 cm forward and 1 cm backward was measured; from these points, an incomplete rectangle delineating the frontal sinus perimeters was drawn. The rectangle area indicates the assumed space of the frontal sinus [20].

Burrow et al. [21] reported that the mean depth of the canine frontal sinus was 2.02–2.49 cm from the lowest to the deepest points. It thus seems to be sufficiently deep for placement of a regular sized fixture. Furthermore, the approach from the rostral side to the canine frontal sinus facilitates a careful manipulation of bone augmentation involving the sinus and scrupulous placement of the dental fixture. Bilateral placements according to different experimental circumstances can be made on both sides of the canine frontal sinus. Although the effect of mastication on the placed site cannot be examined when using the canine frontal sinus, the stability and histological response of the vital bony tissue can be observed without interference from an uncontrolled oral environment (e.g., microorganisms, hygiene conditions, and eccentric occlusion). Selective investigations of the canine frontal and maxillary sinuses might provide data regarding the relative significance of the oral environment, including mastication, on implant placement, in comparison to a group excluding these factors.

Clinically, one of the more important conditions for successful fixture implantation is the primary stability, the cardinal factor underlying which is the residual bone height. The sinus floor elevation for the primary stability in patients with insufficient bone height is generally approached using one of two methods: (1) the osteotome technique, approaching from the occlusal side of the alveolar ridge, and (2) the window-opening procedure, which is performed on the lateral wall of the maxillary sinus [22]. The osteotome technique has been recommended where there is a residual bone height of at least 6–9 mm [23], while the window opening technique is applied when the residual bone height is lower, at 4–5 mm [24]. The similarity of the sinus wall thickness between dogs and humans is very important when considering the significance of experimental results obtained with canine subjects relative to the human condition. Thus, the thickness of the canine frontal sinus is very important information with regard to

experimental dental implant placement. Nevertheless, few studies have investigated the thickness of the canine frontal sinus; our search of the literature revealed only the study of Toyohiko et al. [17], which found that the mean thickness of the frontal sinus wall of beagle dogs was 1.24 mm at one point. In the present study the mean thicknesses of the lateral aspect of the canine frontal sinus wall at 3, 6, 9, 12, and 15 mm lateral to the midsagittal plane were 2.3, 2.7, 3.2, 3.8, and 3.7 mm, respectively. The mean thickness of the canine frontal sinus wall was lowest at 3 mm lateral to the midsagittal plane (2.0–2.2 mm). Yang et al. [25] reported that the mean thickness of the buccofacial wall of the human maxillary sinus was 1.2–1.9 mm. Based on these anatomical data, the window opening procedure on the wall canine frontal sinus could be performed with regard to the procedure on the thickest region of human maxillary sinus [25].

A one-stage procedure with immediate loading was previously suggested only for cases with a residual bone height of >4 mm [26]. However, Peleg et al. [27] reported that the single-stage procedure was also suitable for a residual bone height of <4 mm with adequate primary stability. Moreover, Fugazzotto and Vlassis [28] found that placement of a dental implant with immediate loading where there was a residual bone height of 1–4 mm was successful in 97.0% of cases. However, further histological analysis of the residual bone height condition of <4 mm is needed in animals to establish the efficiency and probability of a successful outcome of immediate loading under these conditions. The mean thickness of the thickest area in this study was 4.0–4.2 mm, while that in the other regions of the sinus was <4 mm (mean thickness 2.0–3.9 mm). Thus, when using the canine frontal sinus model it would be possible to examine the differences in the initial stability of the fixture with immediate loading relative to the bone thickness at multiple sites simultaneously in the same animal.

The maxillary septum acts as a clinical impediment in implant surgery [29]. It has been reported that the presence of septa increases the risk of accidental perforation of the maxillary sinus membrane during the sinus lift procedure [26, 30, 31]. In the present study, the canine frontal sinus was found to be divided into three regions by septa. The rostral and medial portions of the canine frontal sinus were generally very small and occasionally absent. Thus, the presence of septa was irregular between the nasion and the emerging point of the lateral aspect of the canine frontal sinus. Therefore, this model can be used to experimentally evaluate the effect of the

septum at the sinus in the rostral and medial aspects of the canine frontal sinus.

The most common complication during sinus lift surgery is perforation of the maxillary sinus membrane. The mean thickness of the human maxillary sinus membrane has varied widely in previous studies, from 0.1 to 1.0 mm [32-34], whereas that of the canine maxillary sinus membrane ranged from 0.6 to 1.4 mm [35]. Although these values did not match exactly, it has been demonstrated that it is possible to perform appropriate implant surgery experiments on the canine maxillary sinus [15, 16, 35, 36]. Toyohiko et al. [17] also reported that the canine frontal sinus membrane was intact following implantation into the canine frontal sinus wall.

As with the human maxillary sinus, the canine maxillary sinus is known to contain a respiratory epithelium. The normal dog maxillary sinus mucosa is lined with a pseudostratified epithelium [36], and similarly, the epithelial lining of the canine frontal sinus is composed of a pseudostratified ciliated columnar epithelium (PCCE) and goblet cells [37]. The findings of the present study concur with these previous data; the canine frontal sinus membrane was lined with a PCCE, similar to the human maxillary sinus membrane. The ciliated epithelium acts to transport fluids such as pus and mucus. The canine frontal sinus is also relatively resistant to infection. The similarity of the presence of a lining membrane with a ciliated epithelium in the human and dog sinuses supports the acceptability of the canine frontal sinus as a model for studying implant placement and bone augmentation.

In conclusion, the present study has provided some detailed anatomical data regarding the canine frontal sinus, such as its thickness at different regions, and the characteristics of the sinus mucosa, which are pertinent to dental implant research. Furthermore, the findings show that the canine frontal sinus is a suitable alternative model for studying various parameters of sinus augmentation.

References

1. Mayfield LJ, Skoglund A, Hising P, Lang NP, Attström R. Evaluation following functional loading of titanium fixtures placed in ridges augmented by deproteinized bone mineral: a human case study. *Clin Oral Implants Res* 2001;12:508-14.
2. Soncini M, Rodriguez y Baena R, Pietrabissa R, Quaglini V, Rizzo S, Zaffe D. Experimental procedure for the evaluation of the mechanical properties of the bone surrounding dental implants. *Biomaterials* 2002;23:9-17.
3. Bertin PM. The use of multiple implant modalities in the management of the edentulous patient. *Compendium* 1989;10:657-8, 660-1.
4. Bishop K, Addy L, Knox J. Modern restorative management of patients with congenitally missing teeth: 4. The role of implants. *Dent Update* 2007;34:79-80, 82-4.
5. Misch CE. Maxillary sinus augmentation for endosteal implants: organized alternative treatment plans. *Int J Oral Implantol* 1987;4:49-58.
6. van den Bergh JP, ten Bruggenkate CM, Krekeler G, Tuinzing DB. Sinus floor elevation and grafting with autogenous iliac crest bone. *Clin Oral Implants Res* 1998;9:429-35.
7. Kahnberg KE, Ekestubbe A, Gröndahl K, Nilsson P, Hirsch JM. Sinus lifting procedure. I. One-stage surgery with bone transplant and implants. *Clin Oral Implants Res* 2001;12:479-87.
8. Lee SH, Choi BH, Li J, Jeong SM, Kim HS, Ko CY. Comparison of corticocancellous block and particulate bone grafts in maxillary sinus floor augmentation for bone healing around dental implants. *Oral Surg Oral Med Oral Pathol Oral Radiol Endod* 2007;104:324-8.
9. Brumund KT, Graham SM, Beck KC, Hoffman EA, McLennan G. The effect of maxillary sinus anastomosis size on xenon ventilation in the sheep model. *Otolaryngol Head Neck Surg* 2004;131:528-33.
10. Asai S, Shimizu Y, Ooya K. Maxillary sinus augmentation model in rabbits: effect of occluded nasal ostium on new bone formation. *Clin Oral Implants Res* 2002;13:405-9.
11. Bravetti P, Membre H, Marchal L, Jankowski R. Histologic changes in the sinus membrane after maxillary sinus augmentation in goats. *J Oral Maxillofac Surg* 1998;56:1170-6.
12. Hanisch O, Tatakis DN, Rohrer MD, Wöhrle PS, Wozney JM, Wikesjö UM. Bone formation and osseointegration stimulated by rhBMP-2 following subnasal augmentation procedures in nonhuman primates. *Int J Oral Maxillofac Implants* 1997;12:785-92.
13. Haas R, Donath K, Födinger M, Watzek G. Bovine hydroxyapatite for maxillary sinus grafting: comparative histomorphometric findings in sheep. *Clin Oral Implants Res* 1998;9:107-16.
14. Watanabe K, Niimi A, Ueda M. Autogenous bone grafts in the rabbit maxillary sinus. *Oral Surg Oral Med Oral Pathol Oral Radiol Endod* 1999;88:26-32.
15. Liu N, Sun F, Xu C, Lin T, Lu E. A comparative study of dog models for osteotome sinus floor elevation and dental implants in posterior maxilla subjacent to the maxillary sinus. *Oral Surg Oral Med Oral Pathol Oral Radiol* 2013;115:e15-20.
16. Jung JH, Choi BH, Zhu SJ, Lee SH, Huh JY, You TM, Lee HJ, Li J. The effects of exposing dental implants to the maxillary sinus cavity on sinus complications. *Oral Surg Oral Med Oral Pathol Oral Radiol Endod* 2006;102:602-5.
17. Toyohiko H, Takao W, Junichi S. An experimental study on maxillary sinus floor elevation and simultaneous implant placement into the frontal sinus of dogs using bone substitutes. *Tsurumi Shigaku* 2005;31:65-80.
18. Miller ME, Christensen GC, Evans HE. *Anatomy of the dog*. Philadelphia, PA: W. B. Saunders; 1964.
19. Estaca E, Cabezas J, Usón J, Sánchez-Margallo F, Morell E,

- Latorre R. Maxillary sinus-floor elevation: an animal model. *Clin Oral Implants Res* 2008;19:1044-8.
20. Bretan O, Nogueira EA, Silva EF, Trindade SH. Training the osteoplastic flap technique in dogs. *Braz J Otorhinolaryngol* 2005;71:140-4.
 21. Burrow R, McCarroll D, Baker M, Darby P, McConnell F, Cripps P. Frontal sinus depth at four landmarks in breeds of dog typically affected by sinonasal aspergillosis. *Vet Rec* 2012;170:20.
 22. Esfahanizadeh N, Rokn AR, Paknejad M, Motahari P, Daneshparvar H, Shamshiri A. Comparison of lateral window and osteotome techniques in sinus augmentation: histological and histomorphometric evaluation. *J Dent (Tehran)* 2012;9:237-46.
 23. Kolerman R, Moses O, Artzi Z, Barnea E, Tal H. Maxillary sinus augmentation by the crestal core elevation technique. *J Periodontol* 2011;82:41-51.
 24. Del Fabbro M, Corbella S, Weinstein T, Ceresoli V, Taschieri S. Implant survival rates after osteotome-mediated maxillary sinus augmentation: a systematic review. *Clin Implant Dent Relat Res* 2012;14 Suppl 1:e159-68.
 25. Yang HM, Bae HE, Won SY, Hu KS, Song WC, Paik DJ, Kim HJ. The buccofacial wall of maxillary sinus: an anatomical consideration for sinus augmentation. *Clin Implant Dent Relat Res* 2009;11 Suppl 1:e2-6.
 26. van den Bergh JP, ten Bruggenkate CM, Disch FJ, Tuinzing DB. Anatomical aspects of sinus floor elevations. *Clin Oral Implants Res* 2000;11:256-65.
 27. Peleg M, Garg AK, Mazor Z. Predictability of simultaneous implant placement in the severely atrophic posterior maxilla: a 9-year longitudinal experience study of 2132 implants placed into 731 human sinus grafts. *Int J Oral Maxillofac Implants* 2006;21:94-102.
 28. Fugazzotto PA, Vlassis J. Report of 1633 implants in 814 augmented sinus areas in function for up to 180 months. *Implant Dent* 2007;16:369-78.
 29. Beretta M, Cicciù M, Bramanti E, Maiorana C. Schneider membrane elevation in presence of sinus septa: anatomic features and surgical management. *Int J Dent* 2012;2012:261905.
 30. Betts NJ, Miloro M. Modification of the sinus lift procedure for septa in the maxillary antrum. *J Oral Maxillofac Surg* 1994;52:332-3.
 31. Tatum H Jr. Maxillary and sinus implant reconstructions. *Dent Clin North Am* 1986;30:207-29.
 32. Aimetti M, Massei G, Morra M, Cardesi E, Romano F. Correlation between gingival phenotype and Schneiderian membrane thickness. *Int J Oral Maxillofac Implants* 2008;23:1128-32.
 33. Pommer B, Unger E, Suto D, Hack N, Watzek G. Mechanical properties of the Schneiderian membrane *in vitro*. *Clin Oral Implants Res* 2009;20:633-7.
 34. Tos M, Mogensen C. Mucus production in the nasal sinuses. *Acta Otolaryngol Suppl* 1979;360:131-4.
 35. Sul SH, Choi BH, Li J, Jeong SM, Xuan F. Histologic changes in the maxillary sinus membrane after sinus membrane elevation and the simultaneous insertion of dental implants without the use of grafting materials. *Oral Surg Oral Med Oral Pathol Oral Radiol Endod* 2008;105:e1-5.
 36. Choi BH, Zhu SJ, Jung JH, Lee SH, Huh JY. The use of autologous fibrin glue for closing sinus membrane perforations during sinus lifts. *Oral Surg Oral Med Oral Pathol Oral Radiol Endod* 2006;101:150-4.
 37. Abramson AL, Eason RL. Experimental frontal sinus obliteration: long-term results following removal of the mucous membrane lining. *Laryngoscope* 1977;87:1066-73.